

# Comprehensive Assessment of Drug Kinetics, Neurotoxicity, and Safety of Sirolimus-Eluting Intracranial Stents in Canine Basilar Artery

Xuan Sun, MD<sup>\*§</sup>, Xiaojin Wu, BSc<sup>||\*</sup>, Ming Yang, MD<sup>\*§</sup>, Yiming Deng, MD<sup>\*§</sup>, Baixue Jia, PHD<sup>\*§</sup>, Xuelei Zhang, PHD<sup>¶</sup>, Min Zhang, MM<sup>||</sup>, Chaoqiong Pi, MM<sup>||</sup>, Christophe Bureau, PhD<sup>#</sup>, Giuseppina Caligiuri, MD, PhD<sup>††</sup>, Zhongrong Miao, MD<sup>\*§</sup>

<sup>\*</sup>Interventional Neuroradiology, Department of Neurology, Beijing Tiantan Hospital, Capital Medical University, Beijing, China; <sup>§</sup>China National Clinical Research Center for Neurological Diseases, Beijing, China; <sup>||</sup>Sino Medical Sciences Technology Inc. (Sinomed), Tianjin, China; <sup>¶</sup>Department of Cerebrovascular Disease, Beijing Anzhen Hospital, Capital Medical University, Beijing, China; <sup>#</sup>AlchiMedics S.A.S., Paris, France; <sup>††</sup>Department of Cardiology, Université Paris Cité, Laboratory for Vascular Translational Science, INSERM U1148, Bichat University Hospital, Paris, France

\*Xuan Sun and Xiaojin Wu contributed equally to this work.

**Correspondence:** Zhongrong Miao, MD, Interventional Neuroradiology, Department of Neurology, Beijing Tiantan Hospital, Capital Medical University, No. 119, South 4th Ring Rd West, Fengtai District, Beijing, 100070, China. Email: [zhongrongm@163.com](mailto:zhongrongm@163.com)

**Received,** November 23, 2023; **Accepted,** April 30, 2024; **Published Online,** July 10, 2024.

*Neurosurgery* 95:1199–1208, 2024

<https://doi.org/10.1227/NEU.0000000000003079>

© Congress of Neurological Surgeons 2024. All rights reserved.

**BACKGROUND AND OBJECTIVES:** Sirolimus-eluting stents (SESs) have shown promise in treating intracranial atherosclerosis but concerns about potential neurotoxicity due to prolonged drug release exist. The aim of this study was to comprehensively assess the safety of SES, with a focus on neurotoxicity.

**METHODS:** Stents (1.50 × 7 or 12 mm) were implanted into the basilar arteries of 154 Labrador Retrievers (weighing >25 kg and aged older than 1 year) divided into 4 groups: bare-metal stent, polymer-coated stent, standard-dose SES (sirolimus dose: 71 μg), and high-dose SES group (sirolimus dose: 284 μg). Pharmacokinetic analysis was conducted using liquid chromatography-mass spectrometry on blood and tissue samples, and analysis of brain tissue was performed with 5 different special stains and immunohistochemistry protocols to assess axonal degeneration, vacuolization, astrocyte proliferation, microglial activation, or widespread neurodegeneration.

**RESULTS:** In the standard-dose SES group, the stent released 10.56% of the drug on day 1 and 95.41% on day 28 postimplantation. In the high-dose SES group, corresponding figures were 40.20% on day 1 and 98.08% on day 28. Systemic drug concentration consistently remained below 1.5 ng/mL throughout the study. Arterial tissue concentration reached its peak at day 28 days in the standard-dose group and at 7 days in the high-dose group. Importantly, the brain and related tissue concentrations remained below 0.4 μg/g in both standard-dose and high-dose SES groups, peaking on day 21 in the standard-dose group and day 1 in the high-dose group. The detailed 180-day safety assessment revealed no adverse effects on the brain, even at high sirolimus doses in the SES group.

**CONCLUSION:** This study provides robust evidence supporting the long-term pharmacokinetic safety of SESs in the context of intracranial interventions for high-grade intracranial atherosclerosis. The results adequately alleviate concerns related to neurotoxicity and substantiate the feasibility of using these stents as a therapeutic choice in neurosurgery.

**KEY WORDS:** Canine model, Intracranial stents, Pharmacokinetics, Safety assessment, Sirolimus

Intracranial stent deployment reduces stroke risk in patients with intracranial atherosclerotic stenosis but raises concerns about in-stent restenosis (ISR) due to neointimal hyperplasia.<sup>1,2</sup> Drug-

eluting stents (DESs) have emerged as a promising avenue for curtailing ISR and its associated ischemic events by impeding the proliferation and migration of vascular cells poststent deployment.<sup>3-5</sup>

Recently, neurointerventional DES technology advances with improved stent design, polymer chemistry, and drug delivery for enhanced efficacy and safety.<sup>6,7</sup> Sirolimus, an immunosuppressive agent, inhibits vascular cell proliferation and shows promise in managing coronary artery disease.<sup>6</sup> Recent developments created an intracranial sirolimus-eluting stent (SES) system. Clinical trials demonstrate its potential in reducing ISR rates and diminishing

**ABBREVIATIONS:** BMS, bare-metal stent; DES, drug-eluting stent; GFAP, glial fibrillary acidic protein; IBA-1, immunoglobulin binding protein 1; ISR, in-stent restenosis; PBuMA, poly-butyl-methacrylate; PCS, polymer-coated stent; SES, sirolimus-eluting stent.

Supplemental digital content is available for this article at [neurosurgery-online.com](https://neurosurgery-online.com).

recurrent ischemic stroke risk in high-grade intracranial atherosclerotic stenosis.<sup>7</sup>

Nevertheless, concerns persist regarding the potential neurotoxic effects of sirolimus.<sup>8-10</sup> These concerns arise from the brain's unique structural and functional complexity, as well as the specific response of cerebral blood vessels to drugs.<sup>11</sup> Previous studies assessed canine cerebral vasculature and brain tissue histopathology,<sup>12</sup> a precise safety profile customized for brain tissue is lacking. This unmet need is particularly relevant for the utilization of high-dose SESs in patients with intracranial artery stenosis.

## METHODS

### Stent Design

The stents used in this study were intracranial SESs (NOVA, Sinomed Co. Ltd.'s customized device for the trial), composed of 316L stainless steel with a dual-coating system. It consists of a permanent, ultrathin poly-*n*-butyl methacrylate (PBuMA) base layer and a degradable polylactic-polyglycolic acid top coating with sirolimus (1.3 µg/mm<sup>2</sup>) for controlled drug release. The polymer-coated stents (PCS) (Sinomed Co. Ltd.'s customized device for the trial) and the bare-metal stents (BMSs) (Sinomed Co., Ltd.'s customized device for the trial) were used as control stents.

### Experimental Groups and Procedures

154 Labrador Retrievers (older than 1 year, >25 kg, Shanghai Jiagan Biotechnology Co., Ltd.) were divided into 4 groups: BMS, polymer-coated stent (PBuMA PCS, N = 24), standard-dose SES, and high-dose SES. Animals received preoperative aspirin (50 mg once daily, Jiangsu Pingguang Pharmaceutical Co., Ltd.) and clopidogrel (37.5 mg once daily, Aurobindo Pharma USA, Inc.) for 5 days. Initially, a 12-mm stent length was used but caused vessel straightening. To ensure consistency, a 7-mm stent was used for ongoing safety assessment in the standard dose, PBuMA PCS, and BMS groups. Detailed experimental design is shown in **Supplemental Digital Content 1** (<http://links.lww.com/NEU/E365>).

At specified time points, each experimental animal underwent magnetic resonance imaging (Skyra MRI system, Siemens AG) angiography, followed by euthanasia (Zoletil®50, 6 mg/kg, im., Virbac S.A.; Isoflurane, 1%-5%, inhal., RWD Life Science and Technology Co., Ltd.), and the collection of samples for pharmacokinetic evaluation and safety assessment. Analyzed tissues included stented arteries, blood, cerebrospinal fluid (CSF), brain tissue samples from 4 standardized areas (hippocampus, cerebellum, pons, and medulla oblongata) and peripheral organs (kidney, heart, lung, liver, and spleen).

Posteuthanasia, CSF collection involved making a dorsal neck incision extending to the occipital region, exposing the foramen magnum. Blunt dissection separated the dorsal neck muscles for CSF aspiration from the cisterna magna using a syringe and scalpel needle. Subsequently, the skull was opened with an osteotome, and the brain was carefully extracted with forceps to preserve its structure. The brain was photographed, divided into anatomical regions (cerebrum, cerebellum, pons, and medulla oblongata), and documented.

### Pharmacokinetic Evaluation

Drug release kinetics and pharmacokinetics of sirolimus from SES were assessed using liquid chromatography-mass spectrometry. In our

study, drug concentration was analyzed in the basilar artery segment encompassing the stent, measuring 12 mm in length, as well as in the surrounding brain tissues, which included the medulla oblongata, cerebellum, and cerebral bridges. This focused analysis was complemented by histopathological examination of the stent's distal, middle, and proximal segments, and the nonstented vessels located 5 mm from either end of the stent.

For the SES groups, the assessment time points were as follows:

Standard-dose group: Drug release: days 1, 3, 7, 21, 28, 90, and 180; blood/CSF concentration: 5, 30, and 60 minutes, and on days 1, 3, 7, 21, 28, 90, and 180. Arterial, brain, and peripheral tissues: days 1, 3, 7, 21, 28, 90, and 180.

High-dose group: Drug release: days 1, 3, 7, 28, 90, 180, 240, and 300; blood/CSF concentration: 5, 30, 60, and 180 minutes, and on days 1, 3, 7, 28, 90, 180, 240, and 300; brain and peripheral tissues: days 1, 3, 7, 28, 90, 180, and 300.

### Safety Assessment

The safety study followed standard guidelines for evaluating potential neurotoxicity of medical devices.<sup>13</sup> Tissue samples from the brain and peripheral tissues were analyzed using hematoxylin-eosin staining (Hematoxylin-eosin stain, Wuxi Jianguan Industrial Technology and Trade Corporation). Brain samples were additionally stained with Luxol Fast Blue (cresyl violet acetate and solvent blue 38, Sigma-Aldrich Corporation), glial fibrillary acidic protein (GFAP) (anti-GFAP, ab7260, Abcam Trading Co., Ltd.), immunoglobulin binding protein 1 (IBA-1) (anti-IBA-1, ab107159, Abcam Trading Co., Ltd.), Bielschowsky silver (silver nitrate, Sinopharm Chemical Reagent Co., Ltd.), and Fluoro-Jade stains (AG310-30MG, Merck KGaA, Darmstadt [MilliporeSigma]). Digital scanning of microscopic preparations enabled semiquantitative analysis by an independent investigator (Nikon 80i Fluorescence Polarizing Microscope Imaging System, Nikon Corporation). Pathological features were scored on a scale of 1 to 4 based on their extent (<25%, 25%-50%, 50%-75%, >75% of the sample).

The study further conducted behavioral assessments, including (1) respiratory assessment, (2) motor function analysis, (3) convulsion monitoring, (4) righting reflex examination, (5) cardiovascular monitoring, (6) nociceptive response evaluation, and (7) vomiting frequency.

### Assessment of In-Stent Stenosis

Fibrin deposition and stenosis rates were recorded at days 3, 28, 90, and 180 after stent implantations. The area stenosis rate (%) =  $(1 - [\text{lumen area}/\text{internal elastic lamina area}]) \times 100\%$ .

### Statistical Analysis

GraphPad Prism 9.3.1 (GraphPad Software, Inc.) was used for data analysis. Continuous data were presented as means ± SD. Comparisons between 2 groups were conducted using the Wilcoxon matched-pairs signed-rank test (2-tailed). Comparisons involving 3 or 4 groups were performed using 1-way analysis of variance (ANOVA) (for group comparisons) or 2-way ANOVA (considering both group and time effects), with Bonferroni correction. Statistical significance was set at  $P < .05$ .

### Ethic Approval and Informed Consent

This study was approved by the Ethics Committee for animal experiments of PharmaLegacy (Shanghai, China), with the approval numbers PLJC19-0001-A-1, PLJC19-0004-1, and PLJC19-0001-B-1. All animal experiments were performed in accordance with the

Guidelines for the Ethical Review of Laboratory Animal Welfare and approved by the committee on the management and use of laboratory animals of PharmaLegacy.

**Data Availability**

Data supporting article included in article and supplementary materials. Additional data sets became available from corresponding author on reasonable request.

**RESULTS**

Animals were healthy without complications or behavioral abnormalities poststent implantation. MRI showed no significant abnormalities in stented artery morphology or abnormal signals in the brain postimplantation (**Supplemental Digital Content 2**, <http://links.lww.com/NEU/E366>).

**Kinetics of Drug Release from the Stent and Corresponding Concentration in the Cerebral Arteries**

The sirolimus release curves for the standard-dose group were significantly different from those of the high-dose SES group (difference:  $-22.990$ , 95% CI:  $-58.149$  to  $12.169$ ,  $P < .05$ ), as illustrated in Figure 1. In the standard-dose SES group, we observed that 10.56% of the drug was released on day 1, with the final release reaching 95.41% by day 28. By contrast, the high-dose SES group exhibited more pronounced early release, with 40.20% on day 1, and the release progressed somewhat more slowly, finally reaching 98.08% by day 28.

The concentration of sirolimus in the target cerebral arterial tissue consistently peaked at 28 days in the standard-dose group ( $42.8 \pm 38.8 \mu\text{g/g}$ ), coinciding with the completion of stent drug release. Conversely, in the high-dose group, the concentration of sirolimus in arterial tissue reached its peak earlier, at 7 days ( $88.9 \pm 77 \mu\text{g/g}$ ) and

remained significantly higher than in the standard-dose group for up to 28 days when the release from the stent was complete (Figure 2).

**Systemic Drug Levels in the Blood and Cerebrospinal Fluid**

Plasma pharmacokinetics documented consistently low sirolimus concentrations in both groups. In the standard-dose SES group, the maximum level reached was a mere  $1.33 \pm 0.3 \text{ ng/mL}$  at 5 minutes postimplantation, rapidly declining to levels below the lower detection limit ( $<0.1 \text{ ng/mL}$ ) by day 1 (Figure 3). In the high-dose SES group, although exhibiting significantly higher plasma drug concentrations (difference:  $-2.390$ , 95% CI:  $-3.191 \sim -1.589$ ,  $P < .05$ ), maximal levels of  $6.6 \pm 2 \text{ ng/mL}$  were observable between 3 hours and 1 day postimplantation. Subsequently, these concentrations decreased to levels below  $1.5 \text{ ng/mL}$  from day 3 onward and dropped below  $0.1 \text{ ng/mL}$  after 28 days. These markedly low plasma drug levels in both groups, particularly when contrasted with the concentrations detected in cerebral arteries, underscore the effective and controlled release of sirolimus from the NOVA™ SES.

Notably, in the standard-dose SES group, the maximum sirolimus concentration in CSF approached the lower detection limit at  $0.21 \text{ ng/mL}$ . In addition, even in the high-dose SES group, sirolimus levels in the CSF remained considerably low and transient, staying below  $2 \text{ ng/mL}$  (Figure 4).

**Drug Levels in Brain Tissue**

Drug levels reached their peak concentration at the first evaluated time point (1 day) in the high-dose SES group and at day 21 in the standard-dose SES group. However, the peak concentration remained below  $0.4 \mu\text{g/g}$  of tissue in both groups, and time-course differences were not statistically significant. Furthermore, the drug concentrations in the individual brain

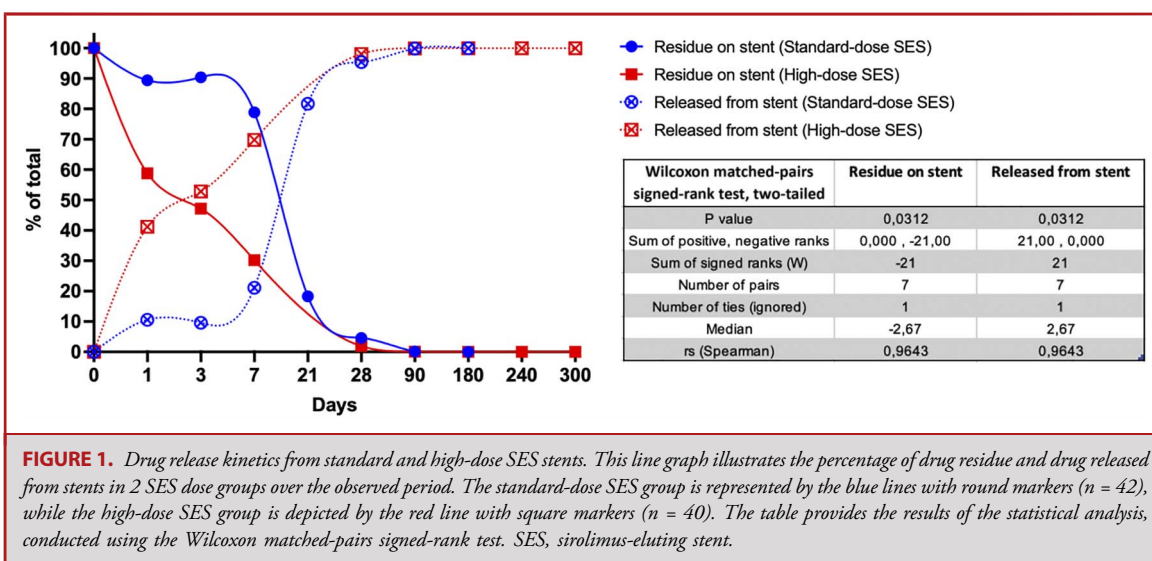


**FIGURE 1.** Drug release kinetics from standard and high-dose SES stents. This line graph illustrates the percentage of drug residue and drug released from stents in 2 SES dose groups over the observed period. The standard-dose SES group is represented by the blue lines with round markers ( $n = 42$ ), while the high-dose SES group is depicted by the red line with square markers ( $n = 40$ ). The table provides the results of the statistical analysis, conducted using the Wilcoxon matched-pairs signed-rank test. SES, sirolimus-eluting stent.

Downloaded from <http://journals.lww.com/neurosurgery> by BHDMSepHKav1Zeum1tQIN4at+KLLHEZgbsHt04XIM0h  
CvWCX1AWNtYQpIIQhD3i3D00dRvT7V5FI4Cj3Vc1y0abgQZxdmwnKZBYws= on 12/01/2024

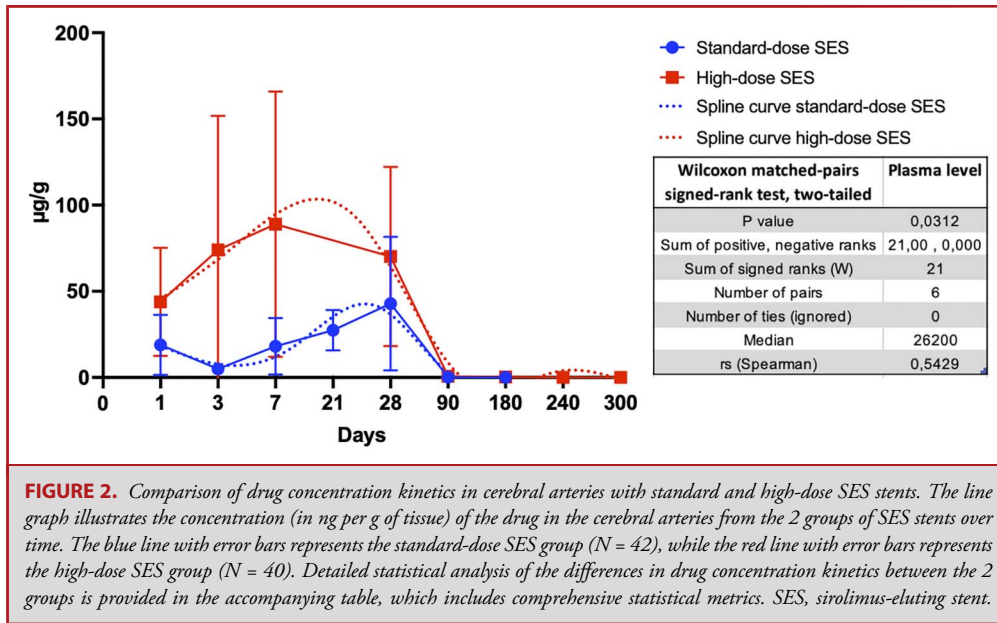


**FIGURE 2.** Comparison of drug concentration kinetics in cerebral arteries with standard and high-dose SES stents. The line graph illustrates the concentration (in ng per g of tissue) of the drug in the cerebral arteries from the 2 groups of SES stents over time. The blue line with error bars represents the standard-dose SES group (N = 42), while the red line with error bars represents the high-dose SES group (N = 40). Detailed statistical analysis of the differences in drug concentration kinetics between the 2 groups is provided in the accompanying table, which includes comprehensive statistical metrics. SES, sirolimus-eluting stent.

areas revealed no significant differences between the 2 groups (Figure 5).

**Drug Levels and Safety Assessment in Peripheral Tissues**

Sirolimus levels in distal organs peaked at a maximum of 20 ng/g on the first day postimplantation in the high-dose SES group, rapidly decreasing through to day 28 and dropping below the detection limit (0.5 ng/g) by day 90 postimplantation. In the

standard-dose SES group, drug concentrations in all examined peripheral tissues consistently remained below 2 ng/g (Figure 6). Organ histopathology analysis showed no significant histopathological changes (data not shown).

**Safety Assessment in Brain Tissues**

Analysis of hematoxylin-eosin preparations at day 3, 28, 90, and 180 after stent implantation revealed that all groups exhibited

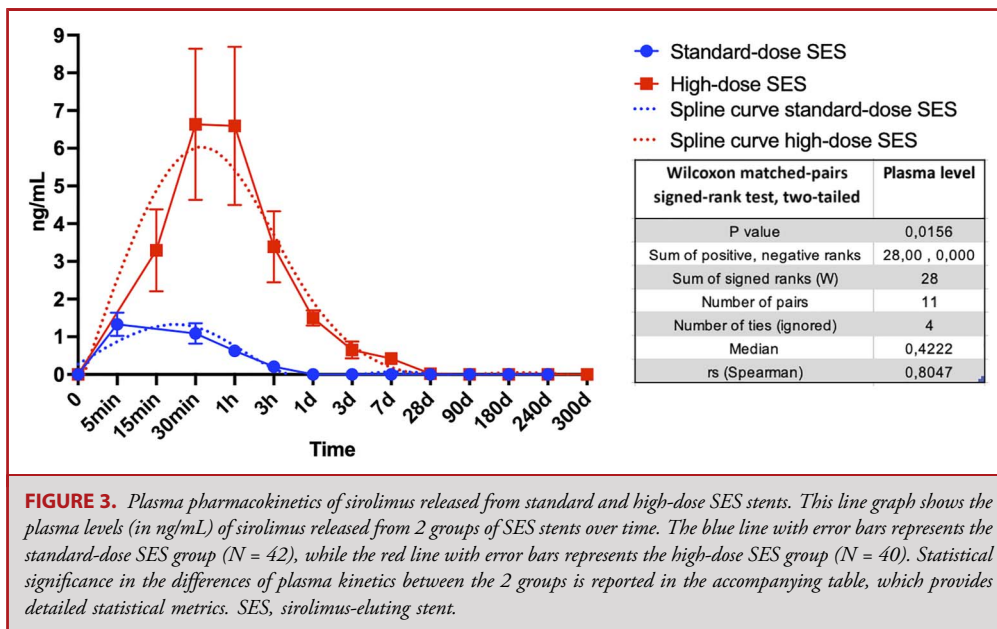


**FIGURE 3.** Plasma pharmacokinetics of sirolimus released from standard and high-dose SES stents. This line graph shows the plasma levels (in ng/mL) of sirolimus released from 2 groups of SES stents over time. The blue line with error bars represents the standard-dose SES group (N = 42), while the red line with error bars represents the high-dose SES group (N = 40). Statistical significance in the differences of plasma kinetics between the 2 groups is reported in the accompanying table, which provides detailed statistical metrics. SES, sirolimus-eluting stent.

Downloaded from http://journals.lww.com/neurosurgery by BHD/MS/EPH/KAV/1ZE/um1Q/N4a+KLLHEZ/bsH/04X/M/0h Cw/CX1AWN/YQp/IIQ/H/D3I3D00d/Ry/7T/VSF/AC/3V/C1y0abgqOZXdwm/KZB/YWS= on 12/01/2024

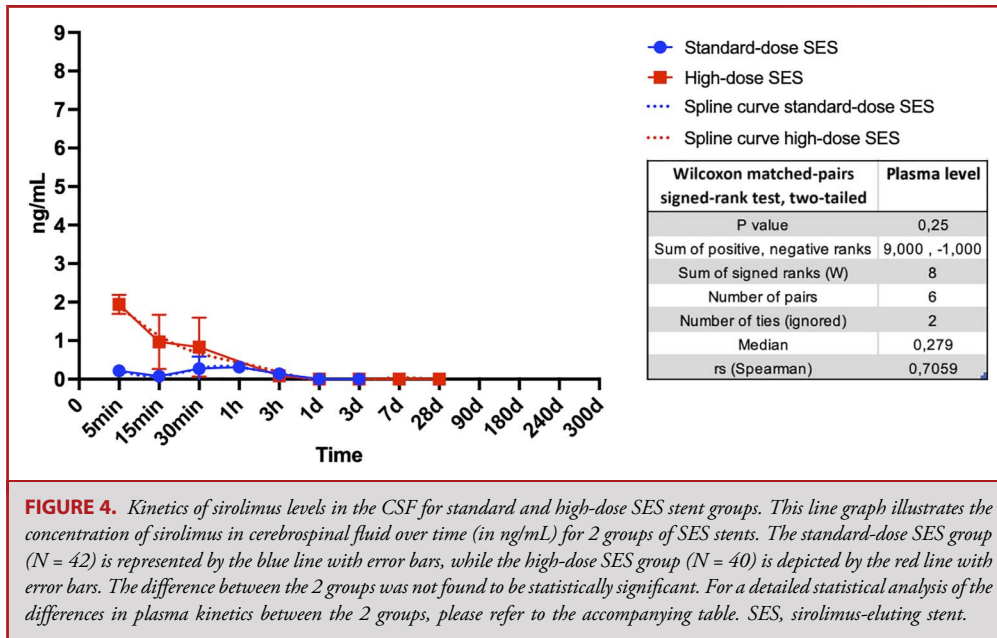


**FIGURE 4.** Kinetics of sirolimus levels in the CSF for standard and high-dose SES stent groups. This line graph illustrates the concentration of sirolimus in cerebrospinal fluid over time (in ng/mL) for 2 groups of SES stents. The standard-dose SES group (N = 42) is represented by the blue line with error bars, while the high-dose SES group (N = 40) is depicted by the red line with error bars. The difference between the 2 groups was not found to be statistically significant. For a detailed statistical analysis of the differences in plasma kinetics between the 2 groups, please refer to the accompanying table. SES, sirolimus-eluting stent.

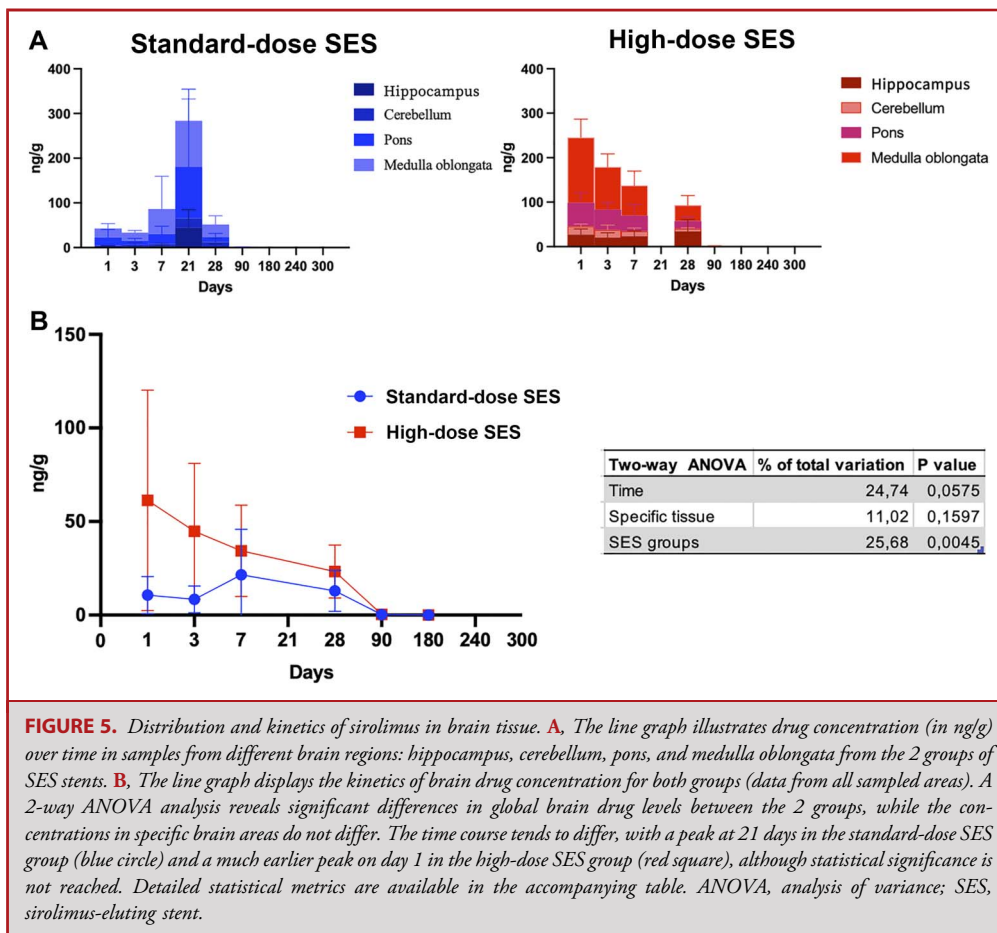


**FIGURE 5.** Distribution and kinetics of sirolimus in brain tissue. **A**, The line graph illustrates drug concentration (in ng/g) over time in samples from different brain regions: hippocampus, cerebellum, pons, and medulla oblongata from the 2 groups of SES stents. **B**, The line graph displays the kinetics of brain drug concentration for both groups (data from all sampled areas). A 2-way ANOVA analysis reveals significant differences in global brain drug levels between the 2 groups, while the concentrations in specific brain areas do not differ. The time course tends to differ, with a peak at 21 days in the standard-dose SES group (blue circle) and a much earlier peak on day 1 in the high-dose SES group (red square), although statistical significance is not reached. Detailed statistical metrics are available in the accompanying table. ANOVA, analysis of variance; SES, sirolimus-eluting stent.

Downloaded from http://journals.lww.com/neurosurgery by BHDMSepHKav1ZEoum1tQIN4at+kLLHEZqbsH04XIM10h CwWCX1AWNyQpIIQhD3i3D00dRy7ITVSFI4C13V1C1y0abgQZXdwmfKZBYms= on 12/01/2024

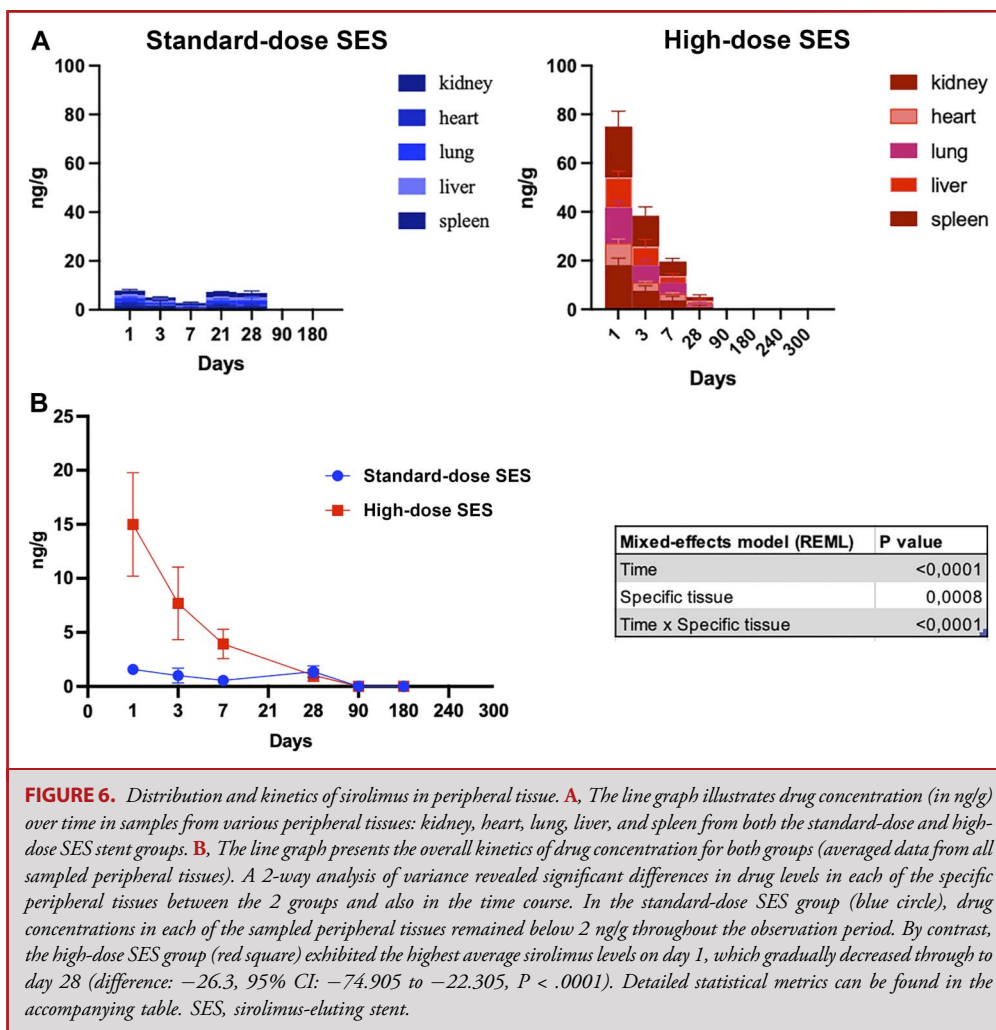


**FIGURE 6.** Distribution and kinetics of sirolimus in peripheral tissue. **A**, The line graph illustrates drug concentration (in ng/g) over time in samples from various peripheral tissues: kidney, heart, lung, liver, and spleen from both the standard-dose and high-dose SES stent groups. **B**, The line graph presents the overall kinetics of drug concentration for both groups (averaged data from all sampled peripheral tissues). A 2-way analysis of variance revealed significant differences in drug levels in each of the specific peripheral tissues between the 2 groups and also in the time course. In the standard-dose SES group (blue circle), drug concentrations in each of the sampled peripheral tissues remained below 2 ng/g throughout the observation period. By contrast, the high-dose SES group (red square) exhibited the highest average sirolimus levels on day 1, which gradually decreased through to day 28 (difference:  $-26.3$ , 95% CI:  $-74.905$  to  $-22.305$ ,  $P < .0001$ ). Detailed statistical metrics can be found in the accompanying table. SES, sirolimus-eluting stent.

only slight signs of tissue degeneration and bleeding and slight-to-moderate hyperplasia. However, the pathological scores were consistently low, and no statistical differences were observed between the groups (**Supplemental Digital Content 3**, <http://links.lww.com/NEU/E367>).

Luxol Fast Blue staining revealed minimal signs of demyelination in a few animals across all groups (**Supplemental Digital Content 4**, <http://links.lww.com/NEU/E368>). GFAP immunostaining showed some astrocyte aggregation in the high-dose group, but the overall staining score remained low (**Supplemental Digital Content 5**, <http://links.lww.com/NEU/E369>). IBA-1 immunostaining indicated slight microglial cell activation, with no significant difference among groups (**Supplemental Digital Content 6**, <http://links.lww.com/NEU/E370>). Bielschowsky silver staining demonstrated occasional axonal degeneration in the medulla oblongata of the high-dose group (**Supplemental Digital Content 7**, <http://links.lww.com/NEU/E371>). Although the difference in axonal degeneration between

groups was statistically significant (difference BMS vs HDS:  $-1.0000$ , 95% CI:  $-1.3227$  to  $-0.6773$ ), difference SDS vs HDS:  $-1.0000$ , 95% CI:  $-1.3227$  to  $-0.6773$ ,  $P < .001$ ), the maximum score consistently remained  $\leq 1$ . These findings provide insights into the potential effects of high-dose SES on various pathological features, warranting further investigation. Fluoro-Jade staining revealed occasional positive neuronal degeneration in the SES groups but without significant difference (**Supplemental Digital Content 8**, <http://links.lww.com/NEU/E372>). However, a significant difference was found in the medulla oblongata after 90 days between high-dose and low-dose groups. No significant differences were observed in other brain tissues among all groups.

### In-Stent Stenosis

Our study results indicated quantifiable changes in fibrin deposition percentages and in-stent stenosis over time (**Supplemental**

**Digital Content 9**, <http://links.lww.com/NEU/E373>). The sirolimus-eluting stent group showed a gradual increase in stenosis rates from  $8.36 \pm 2.61\%$  on day 3 to  $24.76 \pm 7.21\%$  by day 180. Bare-metal stent group showed a slight increase from 9.39% to 20.69%, while polymer-coated stents remained stable at 14.81%. On day 180, the stenosis rates in the SES group were similar to the level in the bare-metal stent group (difference:  $-4.070$ , 95% CI:  $-16.065$  to  $7.925$ ,  $P = .321$ ).

## DISCUSSION

Sirolimus-eluting stents have emerged as a promising option for treating symptomatic high-grade intracranial atherosclerosis.<sup>3,4</sup> However, concerns have been raised regarding potential neurotoxicity due to prolonged rapamycin release. Our study comprehensively assessed the effects of intracranial drug release from standard and high-dose SES on canine cerebral arteries over 180 days, significantly contributing to the emerging field of intracranial arterial revascularization by stenting with SES.

A previous study conducted by Levy et al<sup>12,14</sup> primarily focused on the kinetics of drug release and the response of stented arteries. In that study, the assessment of potential neurotoxicity associated with intracranial SES was limited to hematoxylin and eosin staining. By contrast, our study, with larger sample size and specialized stains, explored neurotoxicity in depth. Importantly, our study confirmed consistent low sirolimus levels in brain tissue, CSF, and peripheral blood after intracranial stent implantation, even with doses higher than those used clinically with NOVA<sup>TM</sup> stents (162  $\mu\text{g}$ ).

As expected, drug release kinetics differed significantly between standard-dose and high-dose groups in early implantation. However, drug release completed within 28 days for both standard and high-dose SES, similar to Supralimus stent (complete release at 48 days).<sup>15</sup>

In our study, sirolimus levels in arterial tissues maintained above minimum effective concentration (1  $\mu\text{g/g}$  tissue) as reported in previous experimental studies,<sup>16,17</sup> while ensuring that concentrations in brain tissue, CSF, systemic circulation, and peripheral tissues consistently below 1  $\mu\text{g/g}$  or 1  $\mu\text{g/mL}$ . The tissue toxicity threshold of sirolimus is not clearly established, but the drug concentrations we found in tissues other than the stented arteries were most likely within safe limits.

In particular, the peak drug concentration in CSF remained considerably below levels associated with *in vitro* neurotoxicity (5  $\mu\text{g/mL}$ ),<sup>18</sup> underscoring the safe and controlled release from the NOVA<sup>TM</sup> stents, even at a 4-fold higher dosage. Importantly, peak sirolimus concentrations in the brain and related tissues consistently remained below 0.4  $\mu\text{g/g}$ , well below the range of 1.7-9.6  $\mu\text{g/g}$ , in which no neurotoxicity was detected in a model involving transient blood-brain barrier opening.<sup>19</sup>

Our study aligns with recent pharmacokinetic research and clinical studies. Sirolimus concentration in arterial tissue peaked on completion of drug release from the stent, at 28 days. By contrast,

arterial tissue concentrations of sirolimus peaked earlier, at 7 days in the high-dose SES group, in alignment with the data reported by Levy et al<sup>12</sup> in a previous comparable study in dogs. Concerning the systemic drug release, our experimental data fairly align with circulating levels of sirolimus observed in patients implanted with Bx Velocity standard and high-dose SES (150  $\mu\text{g}$  and 300  $\mu\text{g}$ , respectively) in human coronary arteries.<sup>20</sup>

Our study was however notably distinct, as it entailed a direct and quantitative evaluation of specific neurotoxicity markers recommended for assessing medical devices intended for permanent implantation in the brain.<sup>13</sup> Our collective findings indicate that sirolimus accumulation in animal brains with high-dose SES implantation caused mild, uniform pathological changes without significant differences among stent groups.

At 90 days, staining scores for medulla oblongata differed significantly between stent groups but not in other brain tissues. The degenerative lesions in the medulla oblongata were mild in the high-dose group. Despite high drug accumulation in the medulla oblongata, canine behavior, respiration, and tissue remained normal in the high-dose group after 180 days. No statistical difference in medulla oblongata tissue after 180 days. Therefore, degenerative lesions at 90 days may not be clinically significant, requiring a larger study for definitive conclusions.

Indeed, given the complexity of access through the canine basilar artery, stent implantation might induce vasospasm and ischemic events, potentially contributing to the observed minimal brain tissue changes. Furthermore, our MRI confirmed the safety of intracranial SES implantation, regardless of the sirolimus dose released from the stent.

In this study, we adjusted drug dosage when modifying stent length. Consistent drug loading per unit area ensured uniform release kinetics, improving precision in pharmacokinetic and safety assessments. However, it is important to acknowledge that changes in stent length can result in variations in overall drug exposure, potentially affecting result accuracy.

Our data suggest that stent obstruction and fibrin deposition are the main causes of in-stent stenosis after implanting stents in normal vessels. The effect of sirolimus on endothelial permeability may increase fibrin deposition on DES, causing higher stenosis rates within 90 days. However, at 180 days, DES and BMS show similar stenosis rates, implying the mitigating effect of sirolimus. This finding aligns with clinical trial showing DES superiority over BMS in reducing ISR rates at the 1-year mark.<sup>7</sup>

## Limitations

Several limitations should be acknowledged. First, our study was conducted in a canine model, and there may be differences in the response of canine cerebral vasculature and brain tissue to SES compared with humans. Second, the brain tissue follow-up period for this study was limited to 180 days, although this is common in such studies. The 180-day observation period showed minimal residual drug and confirmed vascular stability through complete endothelialization. These findings suggest negligible long-term

drug effect, consistent with 1-year trials showing no neurotoxicity.<sup>7</sup> Further studies could extend this time frame to confirm our results. Finally, this study primarily examined pharmacokinetics and histopathological findings. Further research is needed to explore functional or behavioral changes from intracranial sirolimus release.

## CONCLUSION

In conclusion, evaluating histopathological signs of neurotoxicity was justified due to the potential sensitivity of brain cells to sirolimus. Our translational work demonstrates that sirolimus release and metabolism from intracranial stents meet design expectations. Importantly, our long-term safety assessment of SES shows a safety profile similar to bare-metal stents, without any neurotoxic histological signs. These encouraging results significantly advance our understanding of the safety of intracranial DESs, providing essential reassurance to clinicians and researchers concerning their neurological safety.

## Funding

The study was funded by the National Key R&D Program of China (2021YFB3200600, 2021YFB3200604), grant 2016 YFC1301500 from the Ministry of Science and Technology of China (Dr Miao and Dr X. Zhang), Sino Medical Sciences Technology Inc. (Sinomed) (Dr Miao), and National Natural Science Foundation of China (No. 82001247). The funders had no role in study design, data collection, and analysis, decision to publish, or preparation of the manuscript.

## Disclosures

Zhongrong Miao has received a research grant and lecture fee from Sinomed. Xiaojin Wu, Ming Yang, Min Zhang, and Chaoqiong Pi are Sinomed employees. AlchiMedics is a subsidiary of Sinomed. Christophe Bureau is a consultant for Sinomed. Giuseppina Caligiuri is a consultant for AlchiMedics. The other authors have no personal, financial, or institutional interest in any of the drugs, materials, or devices described in this article.

## REFERENCES

- Mohammadian R, Pashapour A, Sharifpour E, et al. A comparison of stent implant versus medical treatment for severe symptomatic intracranial stenosis: a controlled clinical trial. *Cerebrovasc Dis Extra*. 2012;2(1):108-120.
- Peng G, Zhang Y, Miao Z. Incidence and risk factors of in-stent restenosis for symptomatic intracranial atherosclerotic stenosis: a systematic review and meta-analysis. *AJNR Am J Neuroradiol*. 2020;41(8):1447-1452.
- Ye G, Yin X, Yang X, et al. Efficacy and safety of drug-eluting stent for the intracranial atherosclerotic disease: a systematic review and meta-analysis. *J Clin Neurosci*. 2019;59:112-118.
- Kim J, Ban SP, Kim YD, Kwon OK. Long-term outcomes of drug-eluting stent implantation in patients with symptomatic extra- and intracranial atherosclerotic stenoses. *J Cerebrovasc Endovasc Neurosurg*. 2020;22(4):216-224.
- Park S, Lee DG, Chung WJ, Lee DH, Suh DC. Long-term outcomes of drug-eluting stents in symptomatic intracranial stenosis. *Neurointervention*. 2013;8(1):9-14.
- Rosner D, McCarthy N, Bennett M. Rapamycin inhibits human in stent restenosis vascular smooth muscle cells independently of pRB phosphorylation and p53. *Cardiovasc Res*. 2005;66(3):601-610.

- Jia B, Zhang X, Ma N, et al. Comparison of drug-eluting stent with bare-metal stent in patients with symptomatic high-grade intracranial atherosclerotic stenosis: a randomized clinical trial. *JAMA Neurol*. 2022;79(2):176-184.
- Hadamitzky M, Herring A, Kirchhof J, et al. Repeated systemic treatment with rapamycin affects behavior and amygdala protein expression in rats. *Int J Neuropsychopharmacol*. 2018;21(6):592-602.
- Carosi JM, Sargeant TJ. Rapamycin and Alzheimer disease: a double-edged sword? *Autophagy*. 2019;15(8):1460-1462.
- Li XG, Du JH, Lu Y, Lin XJ. Neuroprotective effects of rapamycin on spinal cord injury in rats by increasing autophagy and Akt signaling. *Neural Regen Res*. 2019;14(4):721-727.
- Fisher JA, Mikulis DJ. Cerebrovascular reactivity: purpose, optimizing methods, and limitations to interpretation—a personal 20-year odyssey of (re)searching. *Front Physiol*. 2021;12:629651.
- Levy EI, Hanel RA, Howington JU, et al. Sirolimus-eluting stents in the canine cerebral vasculature: a prospective, randomized, blinded assessment of safety and vessel response. *J Neurosurg*. 2004;100(4):688-694.
- 1670.1-2019 YT. *Evaluation of Neurotoxicity of Medical Devices—PART 1. Standard Guide for Selecting Tests to Evaluate Potential Neurotoxicity*. ICS 1104001.C30.
- Levy EI, Hanel RA, Tio FO, et al. Safety and pharmacokinetics of sirolimus-eluting stents in the canine cerebral vasculature: 180 day assessment. *Neurosurgery*. 2006; 59(4):925-934; discussion 933-924.
- Lemos PA, Bienert I. The Supralimus sirolimus-eluting stent. *Expert Rev Med Devices*. 2013;10(3):295-300.
- Granada JF, Tellez A, Baumbach WR, et al. In vivo delivery and long-term tissue retention of nano-encapsulated sirolimus using a novel porous balloon angioplasty system. *EuroIntervention*. 2016;12(6):740-747.
- Suzuki T, Kopia G, Hayashi S, et al. Stent-based delivery of sirolimus reduces neointimal formation in a porcine coronary model. *Circulation*. 2001;104(10): 1188-1193.
- Serkova N, Christians U, Flögel U, Pfeuffer J, Leibfritz D. Assessment of the mechanism of astrocyte swelling induced by the macrolide immunosuppressant sirolimus using multinuclear nuclear magnetic resonance spectroscopy. *Chem Res Toxicol*. 1997;10(12):1359-1363.
- Cho WS, Choi JH, Kwon OK. Neurotoxicity of paclitaxel and rapamycin in a rat model with transient blood-brain barrier opening. *J Korean Neurosurg Soc*. 2022; 65(2):180-185.
- Otsuka Y, Nakamura M, Yasuda S, et al. Comparison of pharmacokinetics of the sirolimus-eluting stent in Japanese patients with those in American patients. *J Cardiovasc Pharmacol*. 2005;46(4):468-473.

## Acknowledgments

We appreciate PharmaLegacy Labs (Shanghai, China) contributed to this experiment. Author Contributions: Sun, Yang, X Zhang, Wu, M Zhang, and Miao contributed to the research design and interpretation. Sun, Deng, Jia, Wu, M Zhang, and Pi contributed to data collection. Sun and Jia analyzed and interpreted the data. Christophe Bureau and Giuseppina Caligiuri contributed to the draft of the manuscript, analyzed and interpreted the data. Sun, Yang, Wu, and Pi contributed to the draft of the manuscript, which was critically reviewed and revised by Miao. All authors reviewed and approved the final manuscripts.

*Supplemental digital content is available for this article at [neurosurgery-online.com](https://neurosurgery-online.com).*

**Supplemental Digital Content 1. Figure 1.** This figure shows the allocation of the 154 experimental animals to the different stent groups and indicates the groups and samples used for pharmacokinetic evaluation and safety assessment.

**Supplemental Digital Content 2. Figure 2.** Contrast MRI of the brain and cerebral vessels. Contrast MRI was conducted right before termination at each time point to assess the morphology of the basilar artery where the stent was implanted. The images shown in this figure are representative of those taken at day 180 after stent implantation. Sagittal, coronal, and transverse optical sections were obtained through TOF (Time-of-Flight)-3D multislab (multiple thin imaging slices)-MRA (Magnetic Resonance Angiography)-MIP (Maximum Intensity Projection) reconstruction. The reconstructed sections allowed for ruling out gross anatomic pathology by analyzing brain tissue density.



**Supplemental Digital Content 3. Figure 3.** Histopathologic analysis of brain tissue (Hematoxylin-eosin). (a) Representative image of 1 of the analyzed brain areas, the medulla oblongata. (b) Representative high magnification image of the medulla oblongata at day 180 for the 4 groups. Scale bar = 100  $\mu$ m. (c) Quantitative analysis conducted at day 3, 28, 90, and 180 after stent implantation. In each group, 24 animals were included (N = 6 at each time point) for BMS, PCS, and SDS groups, while HDS had 12 animals (N = 3 at each time point). All groups exhibited slight signs of degeneration and bleeding, along with slight-to-moderate signs of hyperplasia and necrosis. Pathological features were scored 1 to 4 based on the extent of these findings (<25%, 25%-50%, 50%-75%, >75% of the sample). The scores were consistently low, with no statistical differences observed between the groups (Groups: BMS—Black squares, PCS—Gray triangles, SDS—Blue circles, HDS—Red squares).

**Supplemental Digital Content 4. Figure 4.** Demyelination analysis (Luxol Fast Blue Staining). (a) Representative image of 1 of the analyzed brain areas, the medulla oblongata. (b) Representative higher magnification images of the medulla oblongata at day 90 for the 3 groups. Scale bar = 100  $\mu$ m. (c) Quantitative analysis performed at day 3, 28, 90, and 180 after stent implantation. The BMS and SDS groups each included 24 animals (N = 6 at each time point), while the HDS group had 12 animals (N = 3 at each time point). Very slight signs of demyelination (appearing as small round vacuoles within the blue matter) were observed in rare animals across all groups. The extent of myelin vacuolization was scored from 1 to 4 (<25%, 25%-50%, 50%-75%, >75% of the sample). The scores consistently remained low, with no statistical differences observed between the groups (Groups: BMS—Black squares, SDS—Blue circles, HDS—Red squares).

**Supplemental Digital Content 5. Figure 5.** Astrocyte Pathology Assessed by GFAP Immunostaining. (a) Representative image of 1 of the analyzed brain areas, the medulla oblongata. (b) Representative higher magnification images of the medulla oblongata at day 90 for the 3 groups. Scale bar = 100  $\mu$ m. (c) Quantitative analysis conducted at day 3, 28, 90, and 180 after stent implantation. The BMS and SDS groups each included 24 animals (N = 6 at each time point), while the HDS group had 12 animals (N = 3 at each time point). Some extent of astrocyte aggregation was observed in the HDS group, but the GFAP staining score consistently remained below 1. Most nerve fibers displayed normal coloring, and no obvious astrocyte proliferation was evident across all groups. The extent of abnormal astrocyte appearance was scored from 1 to 4 (<25%, 25%-50%, 50%-75%, >75% of the sample) (Groups: BMS—Black squares, SDS—Blue circles, HDS—Red squares).

**Supplemental Digital Content 6. Figure 6.** Microglial cell activation assessed by IBA-1 Immunostaining. (a) Representative image of 1 of the analyzed brain areas, the medulla oblongata. (b) Representative higher magnification images of the medulla oblongata at day 180 for the 3 groups. Scale bar = 100  $\mu$ m. (c) Quantitative analysis performed at day 3, 28, 90, and 180 after stent implantation. The BMS and SDS groups each included 24 animals (N = 6 at each time point), while the HDS group had 12 animals (N = 3 at each time point). The extent of positive IBA-1 staining was scored from 1 to 4, representing the percentage of the sample with staining (<25%, 25%-50%, 50%-75%, >75%). While IBA-1 positive staining was slightly more frequent in the HDS group, the difference was not statistically significant, and the maximum score consistently remained at 1 (Groups: BMS—Black squares, SDS—Blue circles, HDS—Red squares).

**Supplemental Digital Content 7. Figure 7.** Axonal degeneration (vacuolization) assessed by Bielschowsky silver staining. (a) Representative image of 1 of the analyzed brain areas, the medulla oblongata. (b) Representative higher magnification images of the medulla oblongata at day 180 for the 3 groups. Scale bar = 100  $\mu$ m. (c) Quantitative analysis performed at day 3, 28, 90, and 180 after stent implantation. The BMS and SDS groups each included 24 animals (N = 6 at each time point), while the HDS group had 12 animals (N = 3 at each time point). Occasional signs of axonal degeneration were observed in the medulla oblongata of the HDS group. Although the difference was statistically significant (1-way ANOVA, difference BMS vs HDS:  $-1.0000$ , 95% CI:  $-1.3227$  to  $-0.6773$ ), difference SDS vs HDS:  $-1.0000$ , 95% CI:  $-1.3227$  to  $-0.6773$ ,  $P < .001$ ), the maximum score consistently remained  $\leq 1$  (on less than 25% of the analyzed sample areas) (Groups: BMS—Black squares, SDS—Blue circles, HDS—Red squares).

**Supplemental Digital Content 8. Figure 8.** Neuronal degeneration assessed by Fluoro Jade staining. (a) Representative images of the analyzed brain areas in the medulla oblongata at day 90 and 180 for the 3 groups. Scale bar = 100  $\mu$ m. (b) Quantitative analysis conducted at day 3, 28, 90, and 180 after stent implantation. The BMS and SDS groups each included 24 animals (N = 6 at each time point), while the HDS group had 12 animals (N = 3 at each time point). Occasional positive staining (green arrow) reflecting neuronal degeneration was observed in the SES groups, but the difference did not reach statistical significance, and the maximum score consistently remained  $\leq 1$  (representing less than 25% of the analyzed areas) (Groups: BMS—Black squares, SDS—Blue circles, HDS—Red squares).

**Supplemental Digital Content 9. Table 1.** Vascular pillar fibrin and stenosis rate assessment at day 3, 28, 90, 180 after stent implantation.

## COMMENTS

This study provides crucial safety data on the use of sirolimus-eluting stents in canine basilar artery. Their results verify concentrations of sirolimus in the brain and circulation to be below toxicity levels, even with high-dose stents. The drug concentrations peak earlier in the high-dose group; however, over 95% of the drug is released by day 28. No evidence of neurotoxicity is seen at a 180-day assessment.

Intracranial atherosclerotic disease (ICAD) accounts for up to 10% of strokes worldwide. Considering over 7 million patients worldwide die from ischemic stroke or its complications each year, ICAD presents a significant disease burden.<sup>1a-4a</sup> Despite these statistics, there is still no effective endovascular treatment for ICAD.<sup>5a</sup> Bare-metal stents (BMSs) have been studied in randomized trials. The results have been dismal. The SAMMPRIS trial showed that Wingspan Stent System (WSS) had high 30-day complication rates (14.7%). Additionally beyond 30 days, WSS did not prevent stroke.<sup>6a</sup> After SAMMPRIS trial results, the FDA and AAN changed their guidelines to recommend stenting with the WSS only after a second stroke while on medical management.<sup>7a</sup> Recently, the CASSISS trial published their results and once again demonstrated that WSS does not reduce the risk of stroke or death when compared with medical therapy alone.<sup>8a</sup> Balloon expandable stent (BES) system in the VISSIT trial was stopped early due to high 30-day primary safety end point in the stenting arm (24.1%).<sup>9a</sup> The repeated failure of BMS may be a result of complicated delivery system and documented high restenosis rates (30%).<sup>10a-12a</sup> This represents a healthcare crisis for over 80 000 patients suffering stroke from ICAD in the United States, since the only humanitarian approved device fails to show promise repeatedly.<sup>5a</sup>

Drug-eluting stents (DESs) are currently the standard of care in coronary literature due to low in-stent restenosis and improved delivery mechanism. However, use in cerebrovascular pathology is limited due to safety concerns of intracranial DES.<sup>13a</sup> In recent years, stent technology has improved significantly and off-label use of DES has increased across the country, demonstrating safe results.<sup>11a</sup> We welcome this safety study as a milestone for development of much needed alternate devices in this empty space.

Sabrina Genovese, Ravi Nunna, and Farhan Siddiq  
Columbia, Missouri, USA

1a. Tsao CW, Aday AW, Almarzooq ZI, et al. Heart Disease and Stroke Statistics—2023 update: a report from the American Heart Association. *Circulation*. 2023; 147(8):e93-e621.

- 2a. Wong LKS. Global burden of intracranial atherosclerosis. *Int J Stroke*. 2006;1(3): 158-159.
- 3a. Gorelick PB, Wong KS, Bae HJ, Pandey DK. Large artery intracranial occlusive disease: a large worldwide burden but a relatively neglected frontier. *Stroke*. 2008; 39(8):2396-2399.
- 4a. GBD 2016 Stroke Collaborators. Global, regional, and national burden of stroke, 1990-2016: a systematic analysis for the Global Burden of Disease Study 2016. *Lancet Neurol*. 2019;18(5):439-458.
- 5a. Sacco RL, Kargman DE, Gu Q, Zamanillo MC. Race-ethnicity and determinants of intracranial atherosclerotic cerebral infarction: the Northern Manhattan stroke study. *Stroke*. 1995;26(1):14-20.
- 6a. Chimowitz MI, Lynn MJ, Derdeyn CP, et al. Stenting versus aggressive medical therapy for intracranial arterial stenosis. *N Engl J Med*. 2011;365(11):993-1003.
- 7a. FDA Safety Communication: Narrowed Indications for Use for the Stryker Wingspan Stent System. <http://www.fda.gov/MedicalDevices/Safety/AlertsandNotices/ucm314600.htm>
- 8a. Gao P, Zhao Z, Wang D, et al. China angioplasty and stenting for symptomatic intracranial severe stenosis (CASSISS): a new, prospective, multicenter, randomized controlled trial in China. *Interv Neuroradiol*. 2015;21(2):196-204.
- 9a. Zaidar OO, Fitzsimmons BF, Woodward BK, et al. Effect of a balloon-expandable intracranial stent vs medical therapy on risk of stroke in patients with symptomatic intracranial stenosis: the VISSIT randomized clinical trial. *JAMA*. 2015;313(12): 1240-1248.
- 10a. Derdeyn CP, Chimowitz MI, Lynn MJ, et al. Aggressive medical treatment with or without stenting in high-risk patients with intracranial artery stenosis (SAMMPRIS): the final results of a randomised trial. *Lancet (London, England)*. 2014;383(9914):333-341.
- 11a. Siddiq F, Nunna RS, Beall JM, et al. Thirty-day outcomes of resolute onyx stent for symptomatic intracranial stenosis: a multicenter propensity score-matched comparison with stenting versus aggressive medical management for preventing recurrent stroke in intracranial stenosis trial. *Neurosurgery*. 2023;92(6):1155-1162.
- 12a. Levy EI, Turk AS, Albuquerque FC, et al. Wingspan in-stent restenosis and thrombosis: incidence, clinical presentation, and management. *Neurosurgery*. 2007;61(3):644-651; discussion 650-651.
- 13a. Abou-Chebl A, Bashir Q, Yadav JS. Drug-eluting stents for the treatment of intracranial atherosclerosis: initial experience and midterm angiographic follow-up. *Stroke*. 2005;36(12):e165-e168.